

**Table 2 Specific heat of X14 propellant and 95% confidence intervals**

$T, ^\circ\text{K}$	$\bar{C}_p, \text{cal/g-K}$	$\bar{C}_p, \text{J/kg-K}$
283	$0.304 \pm 0.013$	$1270 \pm 50$
285	$0.307 \pm 0.012$	$1280 \pm 50$
293	$0.312 \pm 0.014$	$1310 \pm 60$
298	$0.315 \pm 0.013$	$1320 \pm 50$
303	$0.319 \pm 0.017$	$1330 \pm 70$
308	$0.323 \pm 0.015$	$1350 \pm 60$
313	$0.236 \pm 0.016$	$1360 \pm 70$
323	$0.332 \pm 0.018$	$1390 \pm 80$
333	$0.338 \pm 0.016$	$1410 \pm 70$
343	$0.343 \pm 0.016$	$1440 \pm 70$

(DuPont 951) showed a detectable weight loss commencing at 75°C. Kirby and Suh<sup>3</sup> observed a similar phenomenon during heating of another double-base propellant which they attributed to volatilization of the nitroglycerin. The X14 propellant was reweighed at the end of each specific heat determination and showed that no weight change had occurred. All weighings were made with a Cahn RG Electrobalance and all the DSC runs were made in air. The DSC cell is calibrated by running a sample with known specific heat. A sapphire disk in the DSC cell accessory kit is provided for this purpose.

#### Specific Heat Determination

DSC curves of three X14 propellant samples were run from 10°C to 70°C, along with two calibration runs with the sapphire disk. Specific heat at ten temperatures was determined using the following equation

$$\bar{C}_p = \bar{C}_{p_{std}} \times (m_{std}/\Delta Y_{std}) \times (\Delta Y_s/m_s)$$

The results for the three X14 samples and the specific heats used for the sapphire standard are given in Table 1. Table 2 lists the mean specific heat for X14 propellant along with the 95% confidence intervals at each temperature.

Kelley's<sup>4</sup> three-term equation given below was used to algebraically represent the specific heat as a function of temperature.

$$\bar{C}_p = a + bT - cT^{-2}$$

An examination of the specific heats in Table 2 suggested that only the first two terms are necessary to fit the data, so the specific heats in Table 2 were fitted to the previous expression with a nonlinear least squares program<sup>5</sup> with  $c$  set equal to zero. The best-fit values of  $a$  and  $b$  obtained from this calculation are as follows:

$$a = 0.118 \text{ cal/g-K} = 494 \text{ J/kg-K}$$

$$b = 6.60 \cdot 10^{-4} \text{ cal/g-K}^2 = 2.76 \text{ J/kg-K}$$

Table 3 lists the experimental specific heats and the specific heats generated using the best-fit values. In all cases the deviation

**Table 3 Comparison of specific heats generated with best-fits, values of  $a$  and  $b$  with experimental values**

$T, ^\circ\text{K}$	$\bar{C}_p, \text{(expt), cal/g-K}$	$\bar{C}_p, \text{(best-fit), cal/g-K}$
283	0.304	0.305
288	0.307	0.308
293	0.312	0.312
298	0.314	0.315
303	0.319	0.318
308	0.323	0.322
313	0.326	0.325
323	0.332	0.332
323	0.338	0.338
343	0.343	0.345

is well within the 95% confidence intervals, so the two-term equation is deemed adequate to represent the specific heat of X14 from 283-343K.

#### References

- <sup>1</sup> Kirby, C. E. and Suh, N. P., "An Experimental Method for Determining the Condensed Phase Heat of Reaction of Double-Base Propellants," *AIAA Journal*, Vol. 9, No. 2, Feb. 1971, pp. 754-756.
- <sup>2</sup> Baxter, R. A., "A Scanning Microcalorimetry Cell Based on a Thermoelectric Disc-Theory and Application," *Thermal Analysis-Instrumentation Organic Materials, and Polymers*, Edited by R. F. Schwenker and P. D. Garn, Vol. 1, Academic Press, New York, 1969, pp. 65-84.
- <sup>3</sup> Kirby, C. E. and Suh, N. P., "Reactions Near the Burning Surface of Double-Base Propellants," *AIAA Journal*, Vol. 9, No. 4, April 1971, pp. 317-320.
- <sup>4</sup> Kelley, K. K., "Contributions to the Data on Theoretical Metallurgy XIII. High-Temperature Heat-Content, Heat Capacity, and Entropy Data for the Elements and Inorganic Compounds," *U.S. Bureau of Mines Bulletin* 584, 1960.
- <sup>5</sup> Moore, R. H. and Ziegler, R. K., "The Solution of the General Least-Squares Problem with Special Reference to High-Speed Computers," Rept. LA-2367, March 1960, Los Alamos Scientific Lab., Los Alamos, N. Mex.

## Integral Solution of the Turbulent Energy Equation

PAOLO BARONTI\* AND GABRIEL MILLER†

Advanced Technology Laboratories Inc., Westbury, N.Y.

#### Nomenclature

$A, b$	= constants of law of the wall
$a_1, G, L$	= Bradshaw turbulent parameters
$a_4$	= parameter of shear distribution
$u, v$	= velocity components
$x, y, z \equiv y/\delta$	= coordinates
$\tau$	= shear
$\delta, \delta^*$	= thickness and displacement thickness of boundary layer
$c_f$	= skin-friction coefficient
$\pi$	= Coles wake parameter

THE turbulent energy equation in the form proposed by Bradshaw, Ferris and Atwell,<sup>1</sup> namely

$$u \frac{\partial}{\partial x} \left( \frac{\tau}{2a_1\rho} \right) + v \frac{\partial}{\partial y} \left( \frac{\tau}{2a_1\rho} \right) - \frac{\tau}{\rho} \frac{\partial u}{\partial y} + \left( \frac{\tau_{\max}}{\rho} \right)^{1/2} \frac{\partial}{\partial y} \left( \frac{G\tau}{\rho} \right) + \frac{(\tau/\delta)^{3/2}}{L} = 0 \quad (1)$$

lends itself to a simple integral solution, once a representation of shear and velocity profiles through the boundary layer is postulated.

First it is noted that in the vicinity of the wall, production and dissipation are balanced [3rd and 5th term of Eq. (1)]. Then, Eq. (1) can be integrated across the boundary layer from a location  $y_1$  close to the wall to  $\delta$ , to yield

Received June 27, 1973. This Note is part of a research effort on transonic wing design sponsored by ONR under Contract N00014-71-C-0197 and monitored by M. Cooper.

Index category: Boundary Layers and Convective Heat Transfer—Turbulent.

\* Senior Research Scientist. Member AIAA.

† Consultant; also Assistant Professor, New York University, New York. Member AIAA.

$$\int_{y_1}^{\delta} \frac{\partial}{\partial x} \left( \frac{\tau u}{2a_1 \rho} \right) dy - \int_{y_1}^{\delta} \frac{\tau}{\rho} \frac{\partial u}{\partial y} dy + \int_{y_1}^{\delta} \frac{(\tau/\rho)^{3/2}}{L} dy = 0$$

or

$$\frac{d}{dx} (u_e^3 c_f \delta) \int_{\eta_1}^1 \tilde{\tau} \tilde{u} d\eta = (2a_1 u_e^3 c_f) \times \left\{ \int_{\eta_1}^1 \tilde{\tau} \frac{\partial \tilde{u}}{\partial \eta} d\eta - \left( \frac{c_f}{2} \right)^{1/2} \int_{\eta_1}^{\delta} \frac{\tilde{\tau}^{3/2}}{L/\delta} d\eta \right\} \quad (2)$$

where

$$\tilde{\tau} = \tau/\tau_w, \quad \tilde{u} = u/u_e \quad \text{and} \quad \eta = y/\delta$$

The lower integration limit  $\eta_1$  is chosen to lie within the law of the wall region. The shear distribution in the range  $\eta_1 \leq \eta \leq 1$  is represented by the polynomial

$$\tilde{\tau} = a_0 + a_1 \eta + a_2 \eta^2 + a_3 \eta^3 + a_4 \eta^4$$

with the coefficient  $a_0, a_1, a_2, a_3$  provided by the boundary conditions:

$$\tilde{\tau} = \tilde{\tau}_\eta = 0 \quad \text{at} \quad \eta = 1$$

$$\tilde{\tau} = T_1; \quad \tilde{\tau}_\eta = T_2 \quad \text{at} \quad \eta = \eta_1$$

Following Coles,<sup>2</sup> and Rotta,<sup>3</sup> it can be shown,<sup>4</sup> that

$$T_1 = 1 + m_1 \eta_1 + m_2 \left\{ \eta_1 \left[ \ln b \eta_1 \frac{u_e \delta}{\nu} \left( \frac{c_f}{2} \right)^{1/2} - 1 \right]^2 + \eta_1 \right\}$$

$$T_2 = m_1 + m_2 \ln^2 \left[ b \eta_1 \frac{u_e \delta}{\nu} \left( \frac{c_f}{2} \right)^{1/2} \right]$$

where

$$m_1 = -2 \frac{\delta}{c_f} \frac{1}{u_e} \frac{du_e}{dx}; \quad m_2 = A^2 \delta \left( \frac{1}{u_e} \frac{du_e}{dx} + \frac{1}{2} \frac{1}{c_f} \frac{dc_f}{dx} \right)$$

Then, the resulting shear distribution,

$$\tilde{\tau} = \tilde{\tau}(\eta, c_f, u_e, \delta, a_4) \quad (3)$$

should be rather accurate and contain the effects of the flow history through the parameter  $a_4$ . The velocity profiles are prescribed, following Coles,<sup>5</sup> as

$$\tilde{u} = 1 + \left( \frac{c_f}{2} \right)^{1/2} A \{ \ln \eta + 2\pi(3\eta^2 - 2\eta^3 - 1) \} \quad (4)$$

[Coles' wake function  $w(\eta)$  has been approximated by  $2(3\eta^2 - 2\eta^3)$ .]

With Eqs. (3) and (4), the values of  $a_1$  and  $L/\delta$  as given by Bradshaw et al., and after evaluation of the integrals, Eq. (2) becomes an ordinary differential equation in  $a_4(x)$ , assuming that the variables  $u_e, c_f, \delta$  and  $\pi$  are known. In this respect, Eq. (2)

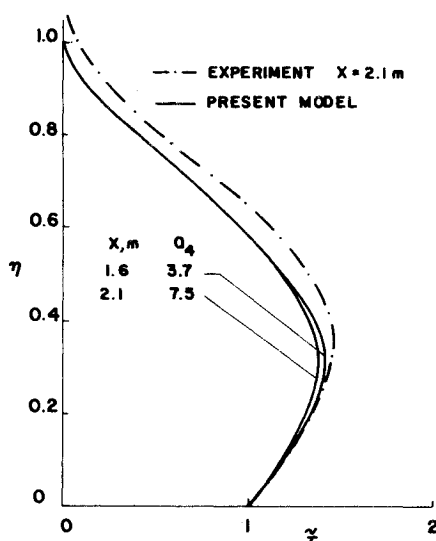


Fig. 1 Development of shear for equilibrium flow of Bradshaw ( $u_e \sim x^{-0.15}$ ), Ref. 6.

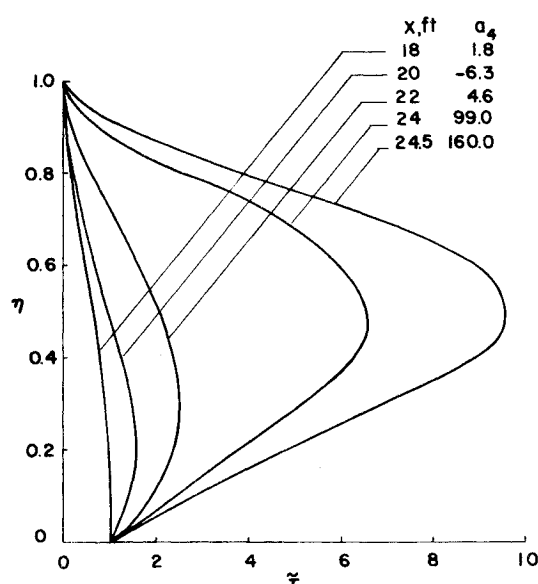


Fig. 2 Development of shear for separating flow of Schubauer and Klebanoff, Ref. 7.

can be used either to determine shear distributions in conjunction with Eq. (3), once  $u_e, c_f, \delta$  and  $\pi$  are given (say by experiments), or, coupled with the continuity and momentum equations (or some integral form thereof), to determine the boundary-layer development.

As typical applications, Figs. 1 and 2 show the development of the shear distribution for one of the equilibrium flows of Bradshaw<sup>6</sup> and for the separating flow of Schubauer and Klebanoff.<sup>7</sup> These results have been obtained by solving numerically Eq. (2) with the values of  $u_e, c_f, \delta$  and  $\pi$  as given by the experiments and reported in Ref. 8, and by taking  $\eta_1 = 0.05$ . It is noted that for the flow of Schubauer and Klebanoff, the point  $\eta_1 = 0.05$  is still within the law of the wall region at the station  $x = 25.4$  ft, which is very close to the point of separation.

An interesting result, relative to the flow of Schubauer and Klebanoff, is the comparison shown in Fig. 3 between the values at  $\eta = 0.5$  of the shears obtained above and the values that may be obtained by assuming a standard eddy viscosity model, that

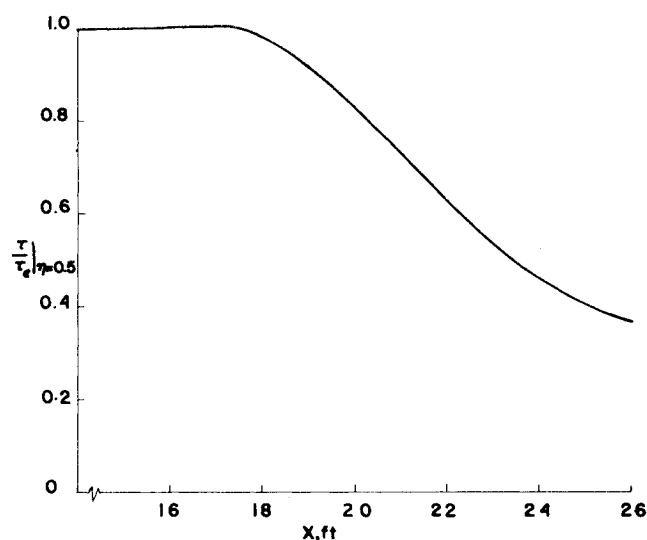


Fig. 3 Shear development in middle of boundary layer for flow of Ref. 7. Comparison of energy solution with eddy viscosity model.

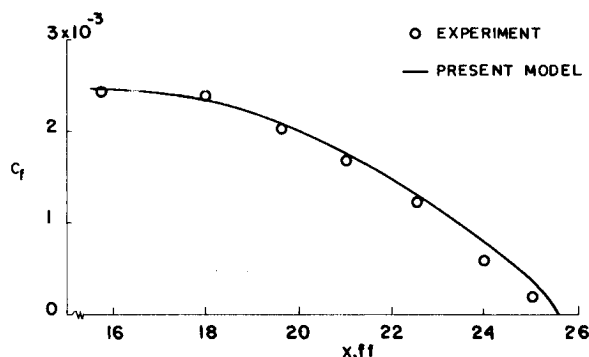


Fig. 4 Prediction of separating flow of Ref. 7.

is, by taking  $\tau_e = 0.016 u_e \delta^* \rho (\partial u / \partial y)$ . Lower values of the shear in the middle of the boundary layer are predicted by use of the energy equation.

A final result shown in Fig. 4 is the theoretical prediction of the separating flow of Schubauer and Klebanoff. For this calculation the integral energy equation, Eq. (2), has been coupled with the integral, two-strip, boundary-layer method of Baronti,<sup>9</sup> which requires specification of the turbulent shear at  $\eta_1 = 0.5$ . The present results appear to be at least as accurate as those obtained by Bradshaw et al. by a finite difference method.

#### References

- Bradshaw, P., Ferris, D. H., and Atwell, M. P., "Calculation of Boundary-Layer Development Using the Turbulent Energy Equation," *Journal of Fluid Mechanics*, Vol. 28, Pt. 3, 1957, pp. 593-616.
- Coles, D., "The Law of the Wall in Turbulent Shear Flow," *Jahre Grenzschichtforsch.*, Vol. 50, 1955, pp. 133-163.
- Rotta, J. C., "The Turbulent Boundary Layers in Incompressible Flow," *Progress in Aeronautical Sciences*, Vol. 2, Pergamon Press, New York, 1962, pp. 1-220.
- Libby, P., Baronti, P. O., and Napolitano, L., "Study of the Incompressible Turbulent Boundary Layer with Pressure Gradient," *AIAA Journal*, Vol. 3, No. 3, March 1964, pp. 445-452.
- Coles, D., "The Law of the Wake in the Turbulent Boundary Layer," *Journal of Fluid Mechanics*, Vol. 1, Pt. 2, July 1956, pp. 191-226.
- Bradshaw, P., "The Turbulence Structure of Equilibrium Boundary Layers," NPL Aero-Rept. 1184, 1966, Aeronautical Research Council, London, England.
- Schubauer, G. B. and Klebanoff, P. S., "Investigation of Separation of the Turbulent Boundary Layer," Rept. 1030, 1951, NACA.
- Coles, D. and Hirst, E. A., "Computation of Turbulent Boundary Layers," *Proceedings of the AFOSR-IFP-Stanford Conference*, Vol. 11, 1968.
- Baronti, P. O., "An Investigation of the Turbulent Incompressible Boundary Layer," GASL TR 624, May 1967, General Applied Science Labs., Westbury, N.Y.

## A Vortex Entrainment Model Applied to Slender Delta Wings

PAUL L. COE JR.\*

Joint Institute of Acoustics and Flight Sciences,  
NASA Langley Research Center, Hampton, Va.

#### Nomenclature

$A$  = wing aspect ratio  
 $a$  = wing semispan at chordwise station  $x$

Received May 5, 1973; revision received September 7, 1973.

Index category: Jets, Wakes, and Viscid-Inviscid Flow Interactions.

\* Assistant Research Professor, George Washington University.

$b$	= wing semispan at trailing edge
$C_L$	= total lift coefficient, $L/\frac{1}{2}\rho U^2 S$
$C_N$	= normal force coefficient, $N/\frac{1}{2}\rho U^2 S$
$c$	= wing chord
$K$	= vortex strength
$K'$	= nondimensional vortex strength, $K/U_c a$
$M$	= sink strength
$M'$	= nondimensional sink strength, $M/U_c a$
$N$	= normal force exerted on wing
$S$	= total wing area
$U$	= freestream velocity
$U_c$	= velocity in cross-flow plane, $U \sin \alpha$
$V$	= resultant velocity along vortex core axis
$V'$	= nondimensional velocity along vortex axis, $V/U_c$
$V'_x, V'_y, V'_z$	= nondimensional components of velocity along vortex axis
$x, y, z$	= body axis coordinate system, Fig. 1
$Z$	= complex variable in cross-flow plane, $z + iy$
$\alpha$	= angle of attack
$\gamma(x)$	= strength per unit width of bound vortex
$\Gamma(y)$	= circulation about spanwise station $y$
$\delta$	= angle of inclination of vortex core above delta wing
$\rho$	= density of fluid
$\zeta$	= complex variable in nondimensional transformed plane, $(Z^2/a^2 + 1)^{1/2}$

#### Introduction

CURRENT experimental studies on bodies of revolution at high angles of attack have shown that the forces and moments developed are greatly affected by the formation of rolled up vortex cores above the lee surface.<sup>1</sup> Thus it is felt that an accurate model of the vortex would aid in the design of fuselage forebodies or slender bodies in general.

Due to geometric simplicity several mathematical models of the vortex flow over a slender, sharp-edged, delta wing have been formulated.<sup>2-5</sup> However, these models generally ignore the entrainment effect of the vortex core, and are found to yield results which are not in agreement with experiment, thus, their extension to the more general case would be of little value.

The technique of Polhamus,<sup>6</sup> referred to as the leading-edge suction analogy, has been found to yield extremely accurate results when compared with experiment. However, there is at present no firm analytical foundation for this result.

It is the intent of this Note to propose a mathematical model of the vortex, which incorporates the previously ignored entrainment effect, and leads to an expression similar to the leading-edge suction analogy.

#### Mathematical Model

Consider a slender, uncambered, sharp-edged, delta wing as shown in Fig. 1. Since vorticity is shed along the entire leading edge, the vortex core is modeled as a line vortex of strength  $K(x)$ . The entrainment of mass by the vortex core is accomplished by superimposing a distribution of sinks along the core axis of strength  $M(x)$ . After being entrained, the mass proceeds along the core axis with velocity  $V$ .

The condition that the line vortex remain stationary is accomplished by requiring that the resultant velocity at the axis of the core be directed along the core axis, as indicated in Fig. 1.

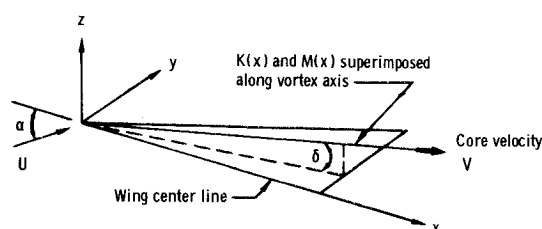


Fig. 1 Illustration of proposed model (half wing shown).